Scientia Iranica D (2013) 20(6), 1999–2014

Sharif University of Technology

Scientia Iranica

Transactions D: Computer Science & Engineering and Electrical Engineering

www.scientiairanica.com

A reliable fault tolerant attitude control system based on an adaptive fault detection and diagnosis algorithm together with a backstepping fault recovery controller

H. Bolandi, M. Haghparast* and M. Abedi

Department of Electrical Engineering, Iran University of Science and Technology, P.O. Box 1684613114, Tehran, Iran.

Received 5 October 2011; received in revised form 2 October 2012; accepted 19 February 2013

KEYWORDS

Fault detection;
Fault isolation;
Fault recovery;
Attitude control;
Hardware in the loop test.

Abstract. This paper presents a practical solution to achieve a fault tolerant attitude control system capable of Fault Detection and Diagnosis (FDD). The novelty of our proposed strategy is in the accurate modeling of satellite dynamics by the Takagi-Sugeno method. Based on this model, an adaptive observer has been utilized to achieve fault diagnosis in reaction wheels of the Attitude Control System (ACS). For this, the occurred faults in reaction wheels have been estimated using an adaptive algorithm which provides fault detection and identification abilities. Moreover, in this paper, a recovery algorithm has been utilized, combined with fault detection and identification algorithm, to provide an advanced decision support system. In this regard, for undertaking the remedial actions, a backstepping feedback linearization control law has been considered in which the estimated fault has been utilized. Accordingly, the boundedness of the attitude control error is guaranteed, despite actuators fault. The developed algorithms provide a significant degree of autonomy to effectively handle satellite operation in the presence of ACS faults, without the ground segment intervention. Through extensive simulation results, the designed algorithms are shown to be robust and accurate. Also, designed algorithms are assessed through hardware in the loop test bed to evaluate their functions in an experimental situation.

1. Introduction

The increasing complexity of satellites, exposure to space radiations and, more importantly, the limited access of satellites cause that fault event in these space vehicles be inevitable. In this regard, although the measures, such as selecting highly reliable components and conducting quality assurance process, make it possible to achieve high reliability, but mentioned strategies only cause delay in fault occurrence [1]. History of fault events in different missions shows thats these events have always been challenging, even in today's modern satellites. A statistical comparison based on data achieved from 1584 satellites between 1984 and 2008 indicates that 36 percent of faults are attributed to the Attitude Determination and Control System (ADCS) [2]. These events have been resulted in degradation of expected services, loss of vehicle control or, in case of total failures, catastrophic loss of mission. Accordingly, there is a need to develop fault tolerance tools in a safety critical subsystem, such as ADCS, capable of detecting, identifying and isolating any component fault.

Traditional Fault Detection and Isolation (FDI) mechanisms are based on hardware redundancy in which the required reliability is achieved by multiple

*. *Corresponding author. Tel.: +98 21 77204040;*
E-mail address: mehran_haghparast@elec.iust.ac.ir (M. Haghparast)

sensors and actuators accompanied by a voting system [3]. In these systems, the value that has the majority in outputs is considered as the desired output value; thus prevents the spread of fault in the system. The Above systems, despite having extensive heritage in aerospace systems, are not suitable solutions for applications in which mass, power and cost are restrictive. The rapid growth of digital implementation techniques have led to a new philosophy in FDI techniques, which are known as analytical redundancy [4]. These approaches are used as a powerful alternative which do not suffer from the restrictions related to mass and power. In fact, analytical methods provide the possibility of replacing the hardware replication with a management of functional or analytical redundancy constituted by the knowledge of system.

Analytical approaches which have been applied to the attitude determination and control system are categorized to model-based and data-based methods [4-7]. In this regard, by using neural networks and available data from a pulsed plasma thruster, this element has been modeled and the output difference of the modeled element and real element has been utilized as a measure for fault detection [8]. Also the authors of [9-11] have used the above method for fault detection. Note that the capabilities of the mentioned approach are restricted only to the range of the stored data, so utilizing this method for a system such as satellite, which may experience unpredicted operational conditions, is risky and may lead to incorrect fault declaration. To deal with the above problem, model-based approaches have been proposed. Kalman filter-based techniques are important model-based methods which have several applications in ADCS. In [12], two Kalman filters have been used for fault detection and isolation which are based on the measured outputs from gyros, sun sensor and magnetometer. Also, the problems of fault detection and isolation based on Extended Kalman Filter (EKF) and Unscented Kalman Filter (UKF) have been addressed for nonlinear dynamics of satellites [13-16]. In [17], application of a bank of interacting multiple Kalman filters for detection and diagnosis of anticipated reaction wheels failures in ACS has been described and developed. Note that, the above method imposes high computational loads, since most of the main modes (dynamics) of the system should be considered in the design process. Also, the modes which are not included cannot be isolated. Kalman filter-based methods, although provide fault detection and isolation capabilities, are not robust against disturbances and uncertainties in the satellite dynamics. To resolve the mentioned problem, an Unknown Input Observer (UIO) has been used in the thrusters of a satellite named MEX to develop fault detection and isolation algorithms which are robust against disturbances [18,19]. Although these algorithms are considered robust techniques against disturbances, they have been applied only for linear dynamics of satellites. The residual generation technique based on H_∞ theory which has been applied for Microscope satellite is also designed for linear dynamics [20]. In contrast, fault detection and isolation methods based on sliding mode observers are an important class of robust techniques which have been applied for nonlinear dynamics of satellites [21-23]. Since, these methods utilize a fixed structure (related parameters cannot be updated online), a conservative upper-bound has been assumed for existing faults and uncertainties in the satellite dynamics. Another approach to compensate the effects of uncertainties and disturbances are adaptive observers, the parameters of which, in contrast to sliding mode, can be updated online, and hence the upper bound of faults and uncertainties is estimated accurately [24,25]. In this approach, the estimated fault term is used as a measure for fault detection and isolation. Adaptive observers applied to ACS, have been designed based on linear dynamics. The scheme developed in this paper, resolve the problem of application of adaptive observers to nonlinear dynamics of satellites. To this end, satellite dynamics has been modeled using Takagi-Sugeno approach which is a new idea in the category of fault diagnosis in ACS. This approach provides the satellite dynamics approximation based on combination of local linear models in different operating points [26]. In this regard, by designing adaptive observer, using the obtained model, the fault occurred in the actuators can be estimated, which in addition to ensuring bounded estimation error, fault detection and identification features are also achieved. On the other hand, for compensating the fault effect and undertaking the appropriate subsequent actions, an active mechanism has been suggested, which provides reconfiguration possibility after fault event. To this end, for ensuring system stability before fault occurrence, backstepping feedback linearization control law has been applied. After fault occurrence, controller structure is reconfigured so that the fault term identified by the adaptive observer is utilized as a compensating factor. Based on the suggested idea, attitude control error remains bounded, even after fault occurrence in reaction wheels. Therefore, the designed recovery algorithm, combined with the fault detection and identification algorithms, provides an advanced decision support system which could expeditiously monitor the system health, and subsequently, appropriate remedial actions are undertaken to maintain the desired specifications. Developed algorithms are assessed through different simulated scenarios. In the simulation model, sensor noises, uncertainties and different space disturbances applied to satellite are modeled. Also, hardware in the loop facility has been developed to qualify the

designed algorithms in the presence of experimental limitations.

The outline of this paper is as follows.: In Section 2, satellite dynamic model is obtained. In Section 3, satellite dynamics is modeled based on the Takagi-Sugeno method. Design of fault detection and identification algorithms are introduced in Section 4. Designed control law for the recovery purposes is included in Section 5. Numerical simulations for a number of faulty scenarios in the reaction wheels are presented in Section 6. In Section 7, hardware in the loop test results, conducted for the purpose of evaluation of the developed algorithms, are described. Finally, conclusions are presented in Section 8.

2. Satellite dynamic model

Before designing the fault detection, identification and recovery algorithms, mathematical model of the attitude control system should be obtained accurately. The satellite considered in this paper is a three axis stabilized satellite in which three reaction wheels are used as actuators. To analyze the satellite motion, three sets of coordinate systems are defined:

1. Earth-centered inertial frame with its origin at the center of the earth, its X_i axis aligned with the vernal equinox, its Z_i axis aligned with the geographic north and its Y_i axis selected such as the above coordinate system becomes right- handed;
2. Body-fixed frame which has its origin at the satellite's center of the mass and its axes (X_b, Y_b and Z_b) aligned with the principal axes of the satellite inertia;
3. Orbital frame which has its origin at the satellite's center of the mass and its Z_o axis points toward the center of the mass of the earth, its X_o axis is in the plane of the orbit, perpendicular to the Z_o axis and in the direction of the satellite velocity and its Y_o axis completes a three-axis right-handed orthogonal system.

The satellite is modeled as a rigid body having the moments of inertia matrix along the principal axes of rotation, $I = \text{Diag}_{3\times 3}\{I_x, I_y, I_z\}$. With the above considerations, satellite attitude dynamics which describes the relations between angular velocities and the applied torques is obtained as follows [27]:

$$\dot{\vec{\omega}} = I^{-1}\left(-\vec{\omega}\times I\vec{\omega} - \vec{\omega}\times I_w\vec{\omega}_w - \dot{h}_W + d\right), \qquad (1)$$

where $\vec{\omega}_{3\times 1}$ is the angular velocity vector of the satellite with reference to the inertial coordinate system, $\vec{\omega}_{w_{3\times 1}} = \begin{bmatrix}\omega_{wx} & \omega_{wy} & \omega_{wz}\end{bmatrix}^T$ is the angular velocity vector of the reaction wheels with reference to the satellite body frame, $\dot{h}_{W_{3\times 1}} = \begin{bmatrix}\dot{h}_{x_w} & \dot{h}_{y_w} & \dot{h}_{z_w}\end{bmatrix}^T$ is the control torque applied to the satellite by the reaction wheels, $I_{w_{3\times 3}} = \text{Diag}_{3\times 3}\{I_{wx}, I_{wy}, I_{wz}\}$ is the moments of inertia matrix of the reaction wheels, d is the disturbance torque which is applied to the satellite and $I_{3\times 3}$ is the moments of inertia matrix of the satellite. Eq. (1) could be stated in the body frame as:

$$\begin{aligned}
\dot{\omega}_x &= \sigma_x\omega_y\omega_z + \frac{I_{wy}\omega_z\omega_{wy} - I_{wz}\omega_y\omega_{wz}}{I_x} - \frac{\dot{h}_{x_W}}{I_x},\\
\dot{\omega}_y &= \sigma_y\omega_x\omega_z + \frac{I_{wz}\omega_x\omega_{wz} - I_{wx}\omega_z\omega_{wx}}{I_y} - \frac{\dot{h}_{y_W}}{I_y},\\
\dot{\omega}_z &= \sigma_z\omega_y\omega_z + \frac{I_{wx}\omega_y\omega_{wx} - I_{wy}\omega_x\omega_{wy}}{I_z} - \frac{\dot{h}_{z_W}}{I_z}, \qquad (2)
\end{aligned}$$

where:

$$\begin{aligned}
\sigma_x &= (I_y - I_z)/I_x,\\
\sigma_y &= (I_z - I_x)/I_y,\\
\sigma_z &= (I_x - I_y)/I_z. \qquad (3)
\end{aligned}$$

In this paper, detection and identification of faults occurred in the reaction wheels have been considered. The main sources and causes of the mentioned faults injected to the reaction wheels are [17]:

- Viscous friction variations;
- Unexpected changes in the satellite bus voltage;
- Unexpected changes in the motor torque values.

In Eq. (4), the fault model occurred in the reaction wheels, due to one or more of the above fault sources, have been proposed. As can be seen, the effect of the mentioned fault sources has been modeled as U_f term in the satellite attitude dynamics.

$$\dot{\vec{\omega}} = I^{-1}\left(-\vec{\omega}\times I\vec{\omega} - \vec{\omega}\times I_w\vec{\omega}_w - \dot{h}_W + U_f + d\right). \qquad (4)$$

As mentioned in Section 1, before designing the fault detection and identification algorithms, nonlinear dynamics of satellite should be modeled using the Takagi-Sugeno method, which is described in the next section.

3. Satellite dynamics modeling based on the Takagi-Sugeno method

The Takagi-Sugeno method is a powerful tool in accurate modeling of nonlinear systems. The useful feature of this method is to build a group of local linear models to describe the original nonlinear systems. As a result, the fault diagnosis schemes for linear systems

can be extended to nonlinear systems. In this section, based on the above idea, satellite dynamics is modeled using local linear dynamics combination. The obtained model is used as a reference model for design of the fault detection and identification algorithms in the next section.

Before describing the satellite attitude dynamics modeling based on the Takagi-Sugeno method, philosophy of this approach is presented for a general nonlinear system. To this end, a smooth time invariant system is considered to be:

$$\dot{x} = f(x,u), \qquad y = g(x), \tag{5}$$

where $x \in R^n$ is the system state variables, $y \in R^p$ is the system output and $f : R^n \times R^m \rightarrow R^n$ and $g : R^n \rightarrow R^p$ are nonlinear smooth vector fields which satisfy Lipchitz conditions.

Takagi-Sugeno method is based on obtaining several local linear models of system and combination of them according to the current operating point. The system model in any of these operating points is stated as [26]:

if $z_1(t)$ is M_1^i, $z_2(t)$ is M_2^i,

and $\cdots z_q(t)$ is M_q^i then:

$$\dot{x}(t) = A_i x(t) + B_i u(t) + \alpha_i,$$

$$y(t) = C_i x(t), \tag{6}$$

where $[z_1(t), z_2(t), \cdots, z_q(t)]$ is the vector of premise variables, $M_1^i, \cdots, M_q^i$ represent fuzzy sets (refer to [28]) and A_i, B_i, C_i and α_i are constant matrices which are obtained by the Jacobean linearization method as [28]:

$$A_i = \frac{\partial f}{\partial x}\Big|_{(x_i,u_i)},$$

$$B_i = \frac{\partial f}{\partial u}\Big|_{(x_i,u_i)},$$

$$C_i = \frac{\partial g}{\partial x}\Big|_{(x_i,u_i)}, \tag{7}$$

in which (x_i, u_i) is the system operating point. Since the points, in which the linearization is done, may not be the system equilibrium points, α_i is utilized to deal with the effect of the system modeling uncertainty:

$$\alpha_i = f(x_i,u_i) - A_i x_i - B_i u_i. \tag{8}$$

The total Takagi-Sugeno fuzzy system is then written as:

$$\dot{x}(t) = \sum_{i=1}^{l} h_i(z)(A_i x(t) + B_i u(t) + \alpha_i) + \Delta f_x,$$

$$y(t) = \sum_{i=1}^{l} h_i(z)(C_i x(t) + c_i) + \Delta f_y, \tag{9}$$

where Δf_x and Δf_y denote respectively the modeling uncertainty and the local linearization uncertainty in the state and output equations, l is the number of fuzzy rules and $h_i(z)$ denotes the weighting coefficient of any of the linear models computed as:

$$h_i(z) = \frac{\mu_i(z)}{\sum_{i=1}^{l} \mu_i(z)}, \qquad \mu_i(z) = \prod_{j=1}^{q} M_j^i(z). \tag{10}$$

In the above equation, the following relation holds for $h_i(z)$:

$$\sum_{i=1}^{l} h_i(z) = 1, \qquad h_i(z) > 0. \tag{11}$$

In nonlinear dynamics modeling of satellite, based on Eq. (2) and (7), the A_i, B_i and C_i matrices are obtained as:

$$A_i = \begin{bmatrix} 0 & \sigma_x\omega_{z_i} - \frac{I_{wz}\omega_{wz_i}}{I_{xx}} & \sigma_x\omega_{y_i} + \frac{I_{wy}\omega_{wy_i}}{I_{xx}} \\ \sigma_y\omega_{z_i} + \frac{I_{wz}\omega_{wz_i}}{I_{yy}} & 0 & \sigma_y\omega_{x_i} - \frac{I_{wx}\omega_{wx_i}}{I_{yy}} \\ \sigma_z\omega_{y_i} - \frac{I_{wy}\omega_{wy_i}}{I_{zz}} & \sigma_z\omega_{x_i} + \frac{I_{wx}\omega_{wx_i}}{I_{zz}} & 0 \end{bmatrix},$$

$$B_i = B = I^{-1} = \begin{bmatrix} 1/I_{xx} & 0 & 0 \\ 0 & 1/I_{yy} & 0 \\ 0 & 0 & 1/I_{zz} \end{bmatrix},$$

$$C_i = C = I_{3\times 3}. \tag{12}$$

Therefore, the vector of $z(t)$ is selected as $[\omega_x(t)\ \omega_y(t)\ \omega_z(t)\ \omega_{wx}(t)\ \omega_{wy}(t)\ \omega_{wz}(t)]$. Also α_i is considered as Eq. (8) for any of the operating points. In this regard, operating point selection for local linearization of satellite is done in a way that covers operational areas of the satellite. So, the satellite dynamics together with the modeling uncertainties can be described as:

$$\dot{\omega}(t) = \sum_{i=1}^{l} h_i(\omega)(A_i\omega(t) + \alpha_i) - B\dot{h}_w(t) + \Delta f_x. \tag{13}$$

Based on Eqs. (4) and (13), attitude control system dynamics, after fault occurrence in actuator(s), is obtained as:

$$\dot{\omega}(t) = \sum_{i=1}^{l} h_i(\omega)(A_i\omega(t) + \alpha_i) - B\dot{h}_w(t) + BU_F(t) + \Delta f_x. \tag{14}$$

Clearly, based on Eq. (12), the output variables are the same as the system state variables, i.e. the angular velocity vector of the satellite.

4. Design of the fault detection and identification algorithms

In this section, design of the fault detection and identification algorithms, based on the obtained Takagi-Sugeno model, is presented. For this, an adaptive fault diagnosis observer is investigated to estimate the angular velocities and accurately reconstruct the fault terms occurred in the reaction wheels. So, using the mentioned idea, it is possible to detect the faults due to actuators, identify them and determine their behavior with reference to time at ACS. The above features which have been achieved by the suggested approach are very critical to provide the required level of satellite autonomy. Especially, it is important to note that the mentioned methodology, proposes a practical solution which can be implemented onboard.

The suggested adaptive observer constructed based on the Takagi-Sugeno model is described by:

$$\dot{\tilde{\omega}} = \sum_{i=1}^{l} h_i(A_i\tilde{\omega} + \alpha_i + L_iC(\omega - \tilde{\omega})) - B\dot{h}_w(t) + B\hat{U}_F(t), \quad (15)$$

where $\widehat{U}_f(t)$ is the fault term estimation and L_i is the observer gain. This gain should be selected such that the convergence of the state estimation errors to zero is guaranteed. Accordingly, the state estimation error dynamics, using the observer presented in Eq. (15) and the system dynamics presented in Eq. (14) is obtained as:

$$\dot{e}_\omega = \sum_{i=1}^{l} h_i(A_i - L_iC)e_\omega + Be_f(t), \quad (16)$$

where $e_\omega(t)$ is the state estimation error of $(\omega - \tilde{\omega})$ and $e_f(t)$ is the actuators fault estimation error of $(U_f(t) - \tilde{U}_f(t))$. Here, it is assumed that the fault is slowly varying. This assumption is due to the fact that in practical conditions, the fault occurred in actuators does not have drastic variations [29]. Therefore, it is obtained that:

$$\dot{e}_f(t) = -\dot{\hat{U}}_F(t). \quad (17)$$

Now, we are ready to present our result which is an adaptive diagnostic algorithm for estimating the fault.

Theory. If there exists a positive definite matrix Π such that:

$$(A_i - L_iC)^T\Pi + \Pi(A_i - L_iC) < 0, \qquad i = 1, 2, \cdots, l, \quad (18)$$

then the observer designed in Eq. (15) and the following adaptive fault estimation algorithm:

$$\dot{\hat{U}}_F(t) = B^T\Pi e_\omega, \quad (19)$$

can realize $\lim_{t\to\infty} e_\omega(t) = 0$ and $\lim_{t\to\infty} e_f(t) = 0$.

Proof. Consider the Lyapunov function $V(t) = e_\omega^T\Pi e_\omega + e_f^T e_f$; its derivative with reference to time is:

$$\begin{aligned}
\dot{V}(t) =& \dot{e}_\omega^T\Pi e_\omega + e_\omega^T\Pi\dot{e}_\omega + \dot{e}_f^T e_f + e_f^T\dot{e}_f \\
=& e_\omega^T \sum_{i=1}^{l} h_i(A_i - L_iC)^T\Pi e_\omega \\
&+ e_f^T B^T\Pi e_\omega + e_\omega^T\Pi \sum_{i=1}^{l} h_i(A_i - L_iC)e_\omega \\
&+ e_\omega\Pi Be_f + \dot{e}_f^T e_f + e_f^T\dot{e}_f \\
=& \sum_{i=1}^{l} h_i e_\omega^T[(A_i - L_iC)^T\Pi + \Pi(A_i - L_iC)]e_\omega \\
&+ e_f^T B^T\Pi e_\omega + e_\omega^T\Pi Be_f + \dot{e}_f^T e_f + e_f^T\dot{e}_f \\
=& \sum_{i=1}^{l} h_i e_\omega^T[(A_i - L_iC)^T\Pi + \Pi(A_i - L_iC)]e_\omega \\
&+ e_f^T B^T\Pi e_\omega + e_\omega^T\Pi Be_f - \dot{\hat{U}}_f^T e_f + e_f^T\dot{\hat{U}}_f. \quad (20)
\end{aligned}$$

From Eqs. (19) and (20) we obtain:

$$\dot{V}(t) = \sum_{i=1}^{l} h_i e_\omega^T[(A_i - L_iC)^T\Pi + \Pi(A_i - L_iC)]e_\omega. \quad (21)$$

Therefore, according to $h_i(\omega) \geq 0$ (Eq. (11)), a sufficient condition for $\dot{V}(t) \leq 0$ is that Eq. (18) is satisfied. So, $\dot{V}(t) \leq 0$ guarantees $\lim_{t\to\infty} e_\omega(t) = 0$ and $\lim_{t\to\infty} e_f(t) = 0$. As a result, the fact $\lim_{t\to\infty} e_f(t) = 0$ makes $\hat{U}_f(t)$ converge to $U_f(t)$ without any estimation error.

This completes the proof. □

A nice feature of the adaptive method proposed in this paper is that the estimation of $\widehat{U}_f(t)$, not only enables fault detection, but also provides the shape of fault which is used for fault accommodation. In an ideal condition in which modeling is considered without uncertainties, $\widehat{U}_f(t)$ term is zero when no faults are present, and this term changes suddenly when the faults occurs. However, since the model has been utilized for attitude control dynamics of the satellite affected by the uncertainties and disturbances, these

factors are also estimated by the adaptive observer together with faults. In other words, the fault estimation accompanies errors due to the mentioned factors. To resolve the above problem, a threshold has been selected, i.e. a fault is declared only if $\widehat{U_f}(t)$ exceeds the selected threshold. Eq. (22) shows the decision making process for the fault declaration:

$$\begin{cases} \left|\hat{U}_f\right| > Tr & \text{Fault occurrence in actuators} \\ \left|\hat{U}_f\right| \leq Tr & \text{No fault occurrence in actuators} \end{cases} \quad (22)$$

where T_r is the threshold for fault declaration, and its value is selected based on: the uncertainties due to the local linear models (Δf_x), the disturbances which are applied to satellite and the accuracy of sensors which measures the angular velocities of satellite. Therefore, based on the designed observer in Eq. (15), it is possible to detect and identify the faults that occur in the actuators.

5. Design of the recovery algorithm

As mentioned before, design of a fault tolerant attitude control system has been considered in this paper to maintain high reliability for satellite control system against possible reaction of wheels faults. This controller provides a solution to meet the desired stability and performance despite the occurrence of faults. So, it is necessary to design a recovery algorithm, in addition to the fault detection and identification algorithms. For this, a control strategy based on the backstepping feedback linearization approach is investigated to ensure the three axis stability of satellite, and then the compensating control law which utilizes the fault estimation is designed to compensate the fault effect. Backstepping method is a recursive scheme, and the idea of it is to design a controller recursively by considering some of the state variables as virtual controls and also to design intermediate control laws for them. To give a clear idea of the above controller, the satellite kinematics relations, considering the orbital frame as reference, are obtained as [27]:

$$\begin{bmatrix} \dot{\phi} \\ \dot{\theta} \\ \dot{\psi} \end{bmatrix} = \begin{bmatrix} \sec\theta \sin\psi\omega_\circ \\ \cos\psi\omega_\circ \\ \sin\phi \sec\theta \sin\psi\omega_\circ \end{bmatrix} + \begin{bmatrix} 1 & \tan\theta\sin\phi & \tan\theta\cos\phi \\ 0 & \cos\phi & -\sin\phi \\ 0 & \sin\phi\sec\theta & \cos\phi\sec\theta \end{bmatrix} \begin{bmatrix} \omega_x \\ \omega_y \\ \omega_z \end{bmatrix}. \quad (23)$$

Eq. (23) together with the satellite dynamic Eqs. (1) can be rewritten as:

$$\dot{E} = S(E,\omega_o) + g(E)\omega,$$
$$\dot{\omega} = D(\omega,\omega_w) - B\dot{h}_W + BU_f, \quad (24)$$

where $E_{3\times1} = \begin{bmatrix}\phi & \theta & \psi\end{bmatrix}$ is the vector of Euler angles, ω_0 is the orbital angular velocity of satellite, $S(E,\omega_o)$ and $g(E)$ are vector fields which can be easily derived from Eq. (23) and D is a nonlinear smooth function as:

$$D = I^{-1}\left(-\vec{\omega}\times I\vec{\omega} - \vec{\omega}\times I_w\vec{\omega}_w\right). \quad (25)$$

The backstepping feedback linearization control law should be designed so that control of the Euler angles vector $E_{3\times1}$, i.e. attitude angles of satellite, is achieved. For this, first, with the assumption of no fault existence in the actuators, two separate steps are considered:

- **Step one:** In this step, due to Eq. (23), ω is considered as input of Eqs. (24), and based on the feedback linearization theory [30] is selected according to Eq. (26). Using this control law provides the convergence of the satellite attitude angles to desired values.

  $$\omega_d = g(E)^{-1}(-S(E) - \Lambda_E(E - E_d) + \dot{E}_d). \quad (26)$$

  In the above equation, $E_{3\times1} = \begin{bmatrix}\phi_d & \theta_d & \psi_d\end{bmatrix}$ is the desired attitude angle of satellite, $\dot{E}_{d_{3\times1}}$ is the desired variation rate of the attitude angles, and $\Lambda_{E_{3\times3}}$ is the design matrix with constant coefficients. If angular velocities of satellite are selected according to Eq. (26), we will have:

  $$\dot{e}_E + \Lambda_E e_E = 0, \quad (27)$$

  in which $e_{E_{3\times1}} = E - E_d$ is the attitude tracking error. Eq. (27) reveals that if $\Lambda_{E_{3\times3}}$ is positive definite, then $E_{3\times1}$ tends to the desired attitude, $E_{d_{3\times1}}$, asymptotically.
- **Step two:** In this step the applied torque to the satellite is designed so that the ω calculated in the first step is achieved. For this purpose, the desired control torque is calculated as follows:

  $$\dot{h}_{W_d} = -B^{-1}(-D(\omega,\omega_w) - \Gamma(\omega - \omega_d) + \dot{\omega}_d), \quad (28)$$

  where ω_d is the desired angular velocity of satellite that was obtained in the first step according to Eq. (26), and $\Gamma_{3\times3}$ is the design constant. If the control torque Eq. (28) is applied to Eqs. (24), we obtain:

  $$\dot{e}_t + \Gamma e_t = 0, \quad (29)$$

  in which $e_{t_{3\times1}} = \omega - \omega_d$ is the angular velocity tracking error, and shows that when no faults exist in the reaction wheels, if $\Gamma_{3\times3}$ is positive definite, then the angular velocities of the satellite tend to the desired angular velocities (Eq. (26)) in a finite time. Considering Eqs. (24), we can rewrite kinematics equations as follows:

  $$\dot{E} = S(E,\omega_o) + g(E)\omega - g(E)\omega_d + g(E)\omega_d = S(E,\omega_o) + g(E)\omega_d + g(E)e_t. \quad (30)$$

Also, according to Eqs. (26) and (27), the attitude tracking error dynamics in the presence of angular velocity tracking error can be written as:

$$\dot{e}_E = -\Lambda_E e_E + g(E)e_t. \tag{31}$$

As Eq. (29) reveals, angular velocity tracking error converges to zero in a finite time. So, defining the augmented error as $e_a = \begin{bmatrix} e_t^T & e_E^T \end{bmatrix}^T$, we obtain:

$$\dot{e}_a = \begin{bmatrix} -\Gamma_{3\times 3} & 0_{3\times 3} \\ g(E(t))_{3\times 3} & -\Lambda_{E_{3\times 3}} \end{bmatrix} e_a. \tag{32}$$

Based on Theorem 8-13 of [31], since Λ_E and Γ are stable and diagonal matrices, the augmented error dynamics is stable if and only if the time varying matrix of $g(E(t))$ is bounded. So the problem of convergence of attitude tracking is turned to evaluating if $g(E(t))$ is bounded or not. Due to Eqs. (26), (31) and (32), three conditions must be considered to guarantee successful tracking:

1. With attention to Eq. (20), $G(E)$ must be bounded. In this regard, Eq. (23) reveals that this condition does not hold just in the singularity point of kinematics at $\theta = 90°$. So the stability condition of system holds in the whole region of system except a single point. The single effect of this singularity is that $\theta_d = 90°$ isn't tractable.
2. According to Eq. (26), $g(E)$ must be invertible. Inverse of this matrix is equivalent to Eq. (33), so it exists and this assumption applies no constrains on the design.

$$g(E)^{-1} = \begin{bmatrix} 1 & 0 & -\sin\theta \\ 0 & \cos\phi & \sin\phi\cos\theta \\ 0 & -\sin\phi & \cos\phi\cos\theta \end{bmatrix}. \tag{33}$$

3. Due to Eq. (31), for a successful attitude tracking, the rate of convergence of the angular velocity tracking error must be much more than the rate of convergence of the attitude tracking error. This requirement is achieved by selecting the proper design coefficients, Λ_E and Γ. For this purpose, the following condition must be held:

$$\text{eigen value}(\Gamma)_i >> \text{eigen value}(\Lambda_E)_i,$$
$$i = x, y, z. \tag{34}$$

This condition guarantees faster tracking of angular velocity rather than the attitude tracking, which leads to a successful attitude tracking.

The occurrence of fault in actuators causes satellite to deviate from the desired attitude. In this condition, the fault term, U_f, appears in the satellite dynamics. So, in the above faulty situations, a compensating algorithm should be activated to tolerate the fault effect and restore the satellite to the desired attitude. In this regard, to handle the fault effect in the actuator(s), a compensating term is added to the control law as [29]:

$$\dot{h}_W = \dot{h}_{W_d} + \dot{h}_{\text{compensation}}. \tag{35}$$

Here, this compensating term is selected as the fault term estimated by the adaptive observer, so we will have:

$$\dot{h}_{\text{compensation}} = \hat{U}_f. \tag{36}$$

Therefore, using the above compensating control law in faulty conditions, the tracking error dynamics of angular velocities with the consideration of Eqs. (24), (28) and (36) is obtained as:

$$\dot{e}_t + \Gamma e_t + B e_f = 0. \tag{37}$$

Defining the new augmented error as $e_{\text{aug}} = \begin{bmatrix} e_f^T & e_t^T & e_E^T \end{bmatrix}^T$, we can write:

$$\dot{e}_{\text{aug}} = \begin{bmatrix} -B^T\Pi & 0_{3\times 3} & 0_{3\times 3} \\ -B & -\Gamma_{3\times 3} & 0_{3\times 3} \\ 0 & g(E(t))_{3\times 3} & -\Lambda_{3\times 3} \end{bmatrix} e_{\text{aug}}. \tag{38}$$

Again, based on Theorem 8-13 of [31], since Λ_E and Γ are stable and diagonal matrices, the augmented error dynamics is stable if and only if the time varying matrix of $g(E(t))$ is bounded, which was discussed before. This equation also applies another condition in the design of Π that $B^T\Pi$ must be positive definite. Attention to the structure of B reveals that this condition is always satisfied. So even in the fault occurrence conditions in the reaction wheels, the satellite tracks its desired attitude.

6. Simulation results

In this section, simulation results of the developed fault detection, identification and recovery algorithms are presented to demonstrate the capabilities of the developed algorithms. These simulations are carried out for a Low Earth Orbit (LEO) satellite, with the altitude 700 kilometers, which has the imaging mission. Satellite moments of inertia are considered $I_{xx} = 4.92$ kgm^2, $I_{yy} = 5$ kgm^2 and $I_{zz} = 1.55$ kgm^2. Also, three reaction wheels aligned with the principal axes of the satellite, and each with the moment of inertia 0.003 kgm^2, are utilized as actuators. For simulation purposes, the effect of disturbances including geomagnetic disturbance torques, gravity gradient disturbances, aerodynamic disturbances and solar radiation disturbances are considered. After analysis and simulation of the above disturbances, a

maximum value, 10^{-5} N.m, has been obtained as their resultant effect, which has been applied in the simulation model. Accordingly, the threshold value is selected as five times of the magnitude of the disturbance value, i.e. 5×10^{-5} N.m. Also, the output error of the sensors for measuring the satellite angular velocities are modeled as a white Gaussian noise with the standard deviation 10^{-5} rad/sec. For modeling the satellite dynamics based on the Takagi-Sugeno method, two operating points of $\left[-\omega_{\max} \quad \omega_{\max}\right]$ for angular velocity and $\left[-\omega_{\text{wheel}_{\max}} \quad \omega_{\text{wheel}_{\max}}\right]$ for rotational velocity of reaction wheels are considered. The maximum velocity of satellite after separation from launcher $\omega_{\max}$ is chosen as 7 deg/sec which is consistent with the data available from different launchers. Maximum value of the reaction wheels velocities depends on their characteristics which here is considered 6000 r.p.m. Also, for each of the components of the angular velocities and reaction wheels velocities, two fuzzy triangular memberships functions $k = x, y, z, M^{\omega_k}_{\text{Negative}}, M^{\omega_k}_{\text{Positive}}$ and $k = x, y, z, M^{\omega_{\text{wheel}_k}}_{\text{Negative}}, M^{\omega_{\text{wh eel}_k}}_{\text{Positive}}$ have been considered. So, the satellite nonlinear dynamics is described with 64 rules. A_i, B_i and C_i matrices are obtained according to Eqs. (12), based on the satellite moments of inertia and assumed operating points. Design matrices $L_i, i = 1, \cdots, 64$ have been obtained using MATLAB, so that Conditions (18) and (30) are satisfied.

For this, after performing various simulations, the above coefficients are tuned so that the suitable responses are achieved. Details of these results are not included here, due to space limitations. Also, design matrices in the controller part are selected as $\Lambda_{E_{3\times3}} = \text{Diag}_{3\times3}\{0.1 \quad 0.1 \quad 0.1\}$ and $\Gamma_{3\times3} = \text{Diag}_{3\times3}\{1 \quad 1 \quad 1\}$. To investigate and study the performance capabilities of the fault detection and identification algorithms, due to the reaction wheels faults, the following three scenarios are considered next:

- *Scenario 1:* In the first scenario, fault does not occur in the reaction wheels. In this scenario, the fault estimation has been presented in Figure 1, and the estimation error of satellite angular velocities has been depicted in Figure 2. These figures reveal that estimation error of the angular velocities is negligible, and the fault estimation in reaction wheels is less than the selected threshold, which has been shown by dash lines. So, as expected, no fault has been declared. As can be observed in Figure 1, the fault estimation is not exactly zero, which may be attributed to the disturbances and noise effects. Also, it is evident that the threshold value has been appropriately and finely selected to avoid false fault declaration.
- *Scenario 2:* In the second scenario, an abrupt fault has been occurred in the reaction wheel, aligned with the x axis, at a time between 200 sec and 250 sec, and with the magnitude 10^{-3} N.m. In these conditions, Figure 3 presents the fault estimation in reaction wheels, and Figure 4 shows the estimation error of angular velocities. The results depicted in Figure 3 imply that only the fault estimation value, aligned with the x axis, has been exceeded the selected threshold, and so, fault is only declared in this axis. Therefore, the designed algorithm has provided the nice feature of isolating the faulty component. Moreover, the fault estimation value, compared to the real value, illustrates that the adaptive observer has the capability to finely and accurately estimate the fault terms. This feature

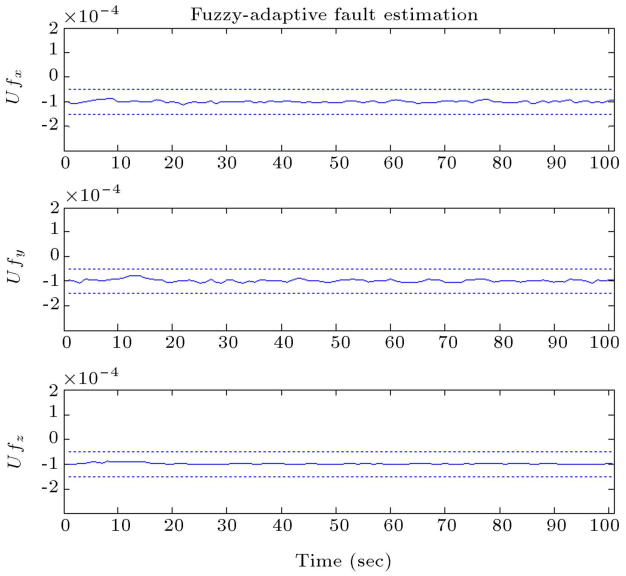

Figure 1. Fault estimation of actuators in the first scenario.

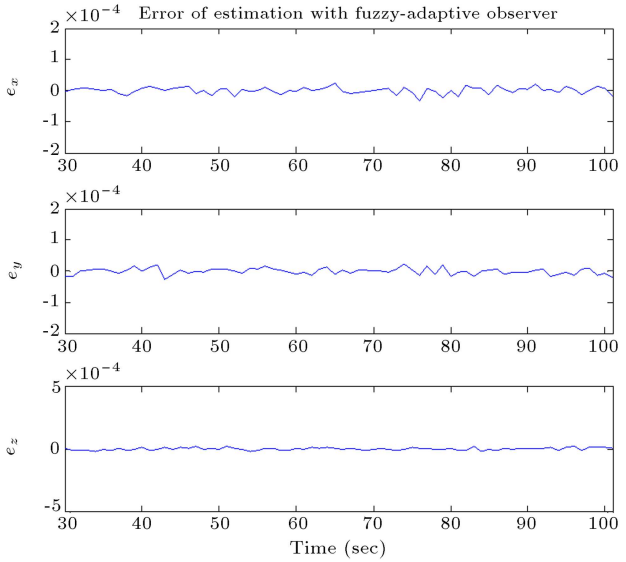

Figure 2. Estimation error of the satellite angular velocities in the first scenario.

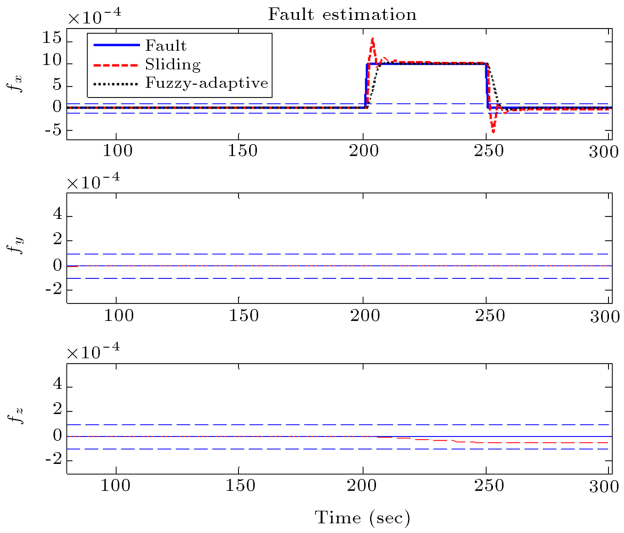

Figure 3. Fault estimation of actuators in the second scenario.

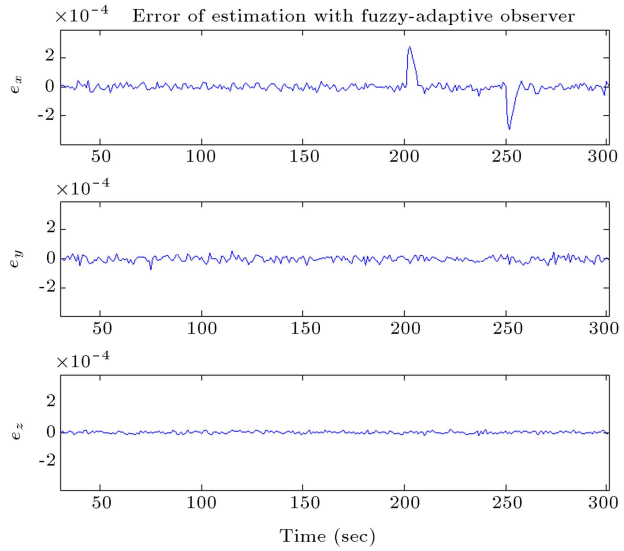

Figure 4. Estimation error of the satellite angular velocities in the second scenario.

leads to the boundedness of the estimation error of angular velocities, despite the fault occurrence in the reaction wheels. This error deviates only in the fault occurrence times which damps immediately. Note that in Figure 3, performance of the developed method has been compared with a fault estimator based on the Sliding Mode Observer (SMO) [21,23]. As shown in this figure, the fault estimated by the Fuzzy-Adaptive Observer (FAO) represents an overshoot of 1.7%, settling time of 13 sec and estimation error of 0.1%; however, the SMO method provides an overshoot of 55%, the settling time of 28 sec and the estimation error of 2%.

- *Scenario 3:* To further substantiate the FDD algorithm robustness, in this scenario, incipient faults with the slope 10^{-5} N.m have been applied in all three reaction wheels. The Above faults have occurred at 200 sec. In this regard, Figure 5 shows the fault estimation in reaction wheels, and the estimation error of angular velocities has been depicted in Figure 6. As can be seen in Figure 5, the fault estimation in all three axes violates the selected threshold at a considered time interval, which verifies the performance of the fault detection algorithm. Also, it reveals that the fault magnitudes are accurately estimated. Figure 6 shows that the estimation error of angular velocities is bounded in spite of fault occurrence, which attributed to the fault estimation capability of the adaptive observer. Note that in Figure 5, performance of the devel-

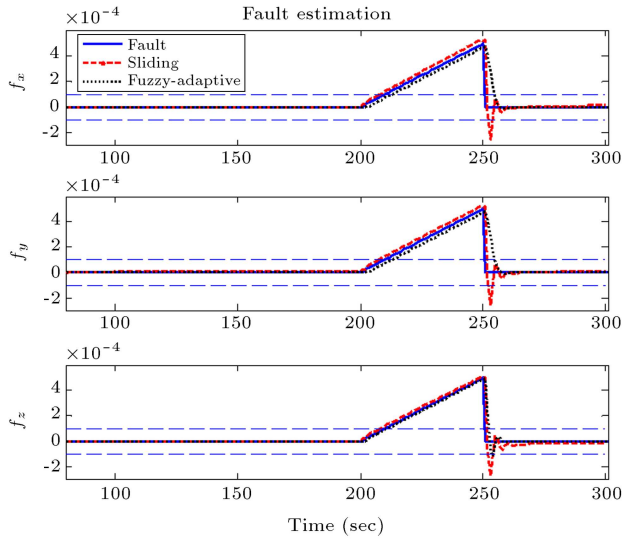

Figure 5. Fault estimation of actuators in the third scenario.

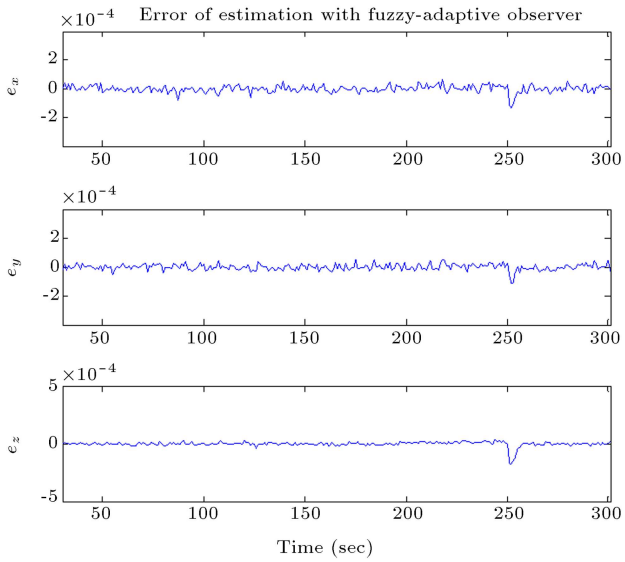

Figure 6. Estimation error of the satellite angular velocities in the third scenario.

Table 1. Performance of the proposed method in comparison to the sliding mode observer approach.

	Fault detection time		Overshoot		Settling time		Fault estimation accuracy		Sensitivity to sample rate	
Fault type	**SMO**	**FAO**	**SMO**	**FAO**	**SMO**	**FAO**	**SMO**	**FAO**	**SMO**	**FAO**
Abrupt	2.1 sec	2.5 sec	55%	1.7%	28 sec	13 sec	2%	0.1%	High	Normal
Incipient	10 sec	12 sec	—	—	—	—	4.6%	1.9%	High	Normal

oped method has been compared with the SMO. It can be seen that the estimation error of 1.9% is attained using the developed method; however, an estimation error of 4.6% is provided by the SMO method. Similarly, by carrying out simulations for different scenarios, effectiveness of the proposed fault detection, isolation and identification algorithms is demonstrated. The associated graphs are not shown here for brevity.

Table 1 summarizes the results obtained by the FAO in comparison to the SMO. According to this table, although the fault detection times, provided by the outlined methods, are almost close to each other (sliding mode estimator yields a somewhat better performance), the estimation accuracy achieved by the FAO is significantly better than the SMO. Also, our investigations show that the SMO approach is more sensitive to the sampling time variations. Accordingly, the estimation ability attained, using the FAO, provides a better match, compared to the real fault value. The outlined ability is especially important about the compensators which use the estimated fault term to maintain the system stability. In fact, a more accurate fault estimation can eventually lead to a more robust remedial action.

Next step is verification of the recovery algorithm. For this purpose, satellite attitude error is shown in Figure 7. As can be observed from this simulation, the value 0.0062 deg has been obtained as the pointing accuracy in presence of noise and disturbance torques. So, it reveals that an acceptable orientation response has been achieved by the backstepping feedback linearization control law, and the satellite has reached the desired angle. Now, performance of the recovery algorithm is investigated against abrupt faults with the magnitude 10^{-3} N.m, which are introduced in all three reaction wheels at 120 sec. For this, Figure 8 depicts the satellite attitude errors about the roll, pitch and yaw axes, in which the compensator controller has not been utilized. Based on the obtained results, tracking errors 147 deg about the yaw axis, 0.44 deg about the pitch axis and 0.47 deg about the roll axis have been gained. So, the system performance is significantly degraded after actuator faults, which may lead to undesired effects on mission imaging resolution.

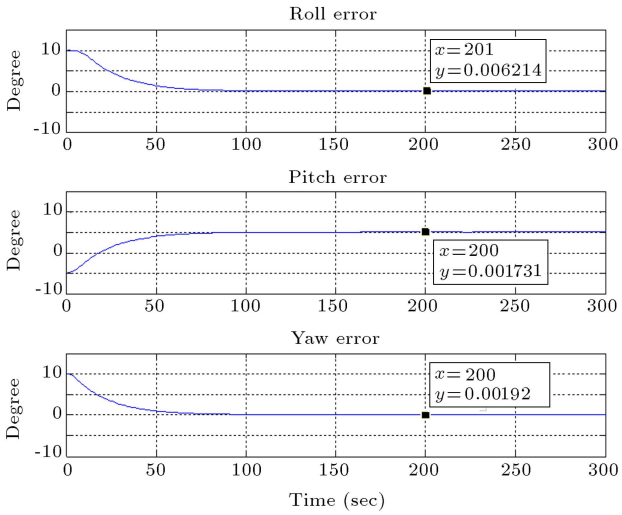

Figure 7. Attitude errors about the roll, pitch and yaw axes in case of no fault occurrence at the satellite reaction wheels and without fault compensation.

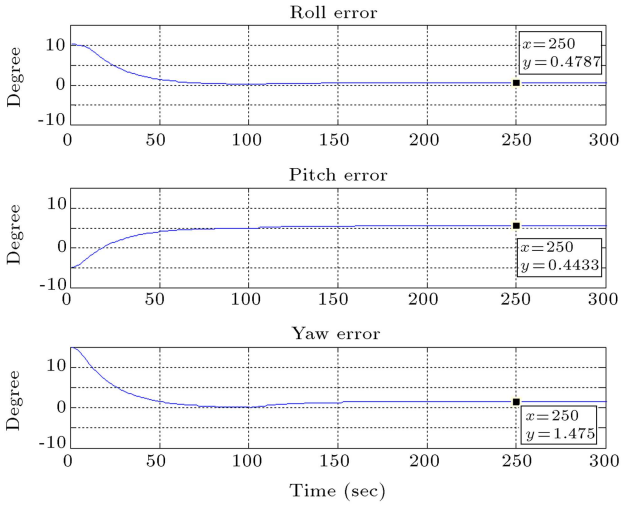

Figure 8. Attitude errors about the roll, pitch and yaw axes in case of fault occurrence at the satellite reaction wheels and without fault compensation.

Moreover, occurrence of an abrupt fault with a larger magnitude or an intermittent fault may lead to a more severe effect or even loss of the satellite control.

Therefore, the necessity of utilizing a compensator controller, together with the designed algorithm is evident. With activation of the compensator controller,

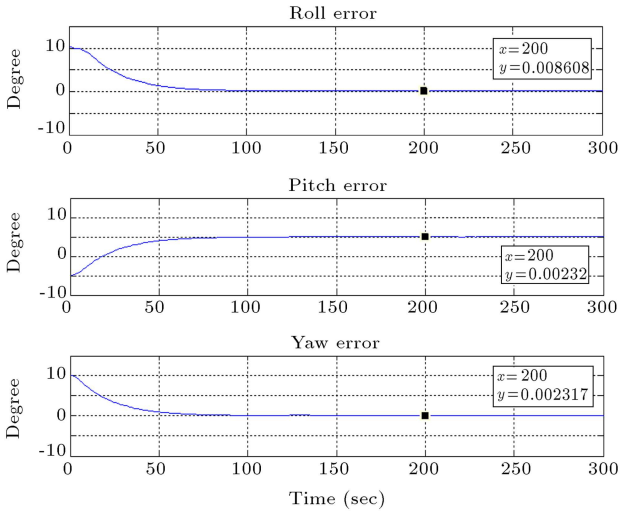

Figure 9. Attitude errors about the t roll, pitch and yaw axes in case of fault occurrence at the satellite reaction wheels and together with fault compensation.

the satellite attitude errors have been illustrated again in Figure 9. It can be seen that high control precision and a good tracking process are still obtained, despite fault existence in actuators and deviation of their generated control torques from the desired values. So, the satellite maintains the desired attitude, and effectiveness and applicability of the recovery algorithm are verified. Summarizing all the cases, it is noted that the proposed adaptive observer provides fault identification with an acceptable accuracy. Utilizing this capability combined with the threshold selection process leads to a high reliability attributed to the fault detection and identification processes.

Another important merit of the designed algorithm is that in case of fault occurrence in an actuator, only the fault term associated with that actuator violates the selected threshold, which typically provides the fault isolation capability. Simulation results also show that the recovery algorithm can significantly improve the normal performance mode, and so this feature together with the outlined fault detection, isolation and identification capabilities achieves an automatic and independent fault tolerant attitude control system.

7. Hardware In the Loop (HIL) test

To evaluate the potentialities of utilizing the proposed algorithms in real applications, and investigate their capability to onboard implementation, in this section, the results of the Hardware In the Loop (HIL) tests are presented. These experimental results validate the desired requirements attributed to the designed algorithms considering the real conditions, which the satellite may experience in the orbital situations. For this, hardware in the loop test bed is planned according to Figure 10, which provides the ability to test Fault Detection, Isolation and Recovery (FDIR) algorithms

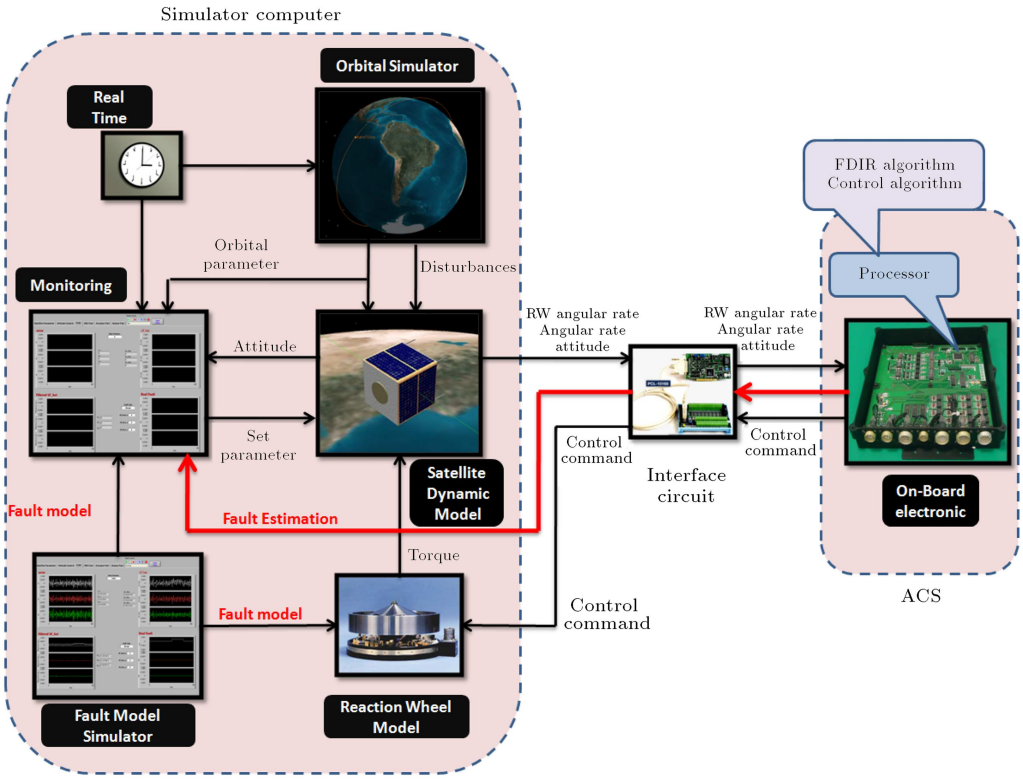

Figure 10. Different elements of the hardware in the loop test bed.

in close to a real-time condition. This facility includes the following main elements:

- *Simulator computer*: this simulator which has been created by the lab view software provides the possibility to accurately model the satellite dynamics, considering the factors such as uncertainties, space disturbances, sensor noise and reaction wheel models. In this environment, we also have the fault simulator to monitor the parameters related to the FDIR algorithms, and analyze their performance. The simulator computer also provides a special monitoring environment to track the control algorithms, their generated moments which apply to the satellite, and the angular rates which have been achieved by them.
- *On-board electronics*: the fault detection, identification and recovery algorithms have been implemented in this element. The processor utilized in this product is selected from the 8051 family which, in addition to satisfy our technical specifications, has a history of use in different space missions. This element also provides the flexibility to implement and evaluate different attitude control and FDIR algorithms. As seen from Figure 10, the onboard electronics receives the satellite attitude, satellite angular rates and reaction wheel angular rates as its input states, and after process and execution of the implemented FDIR algorithms, generates the torque commands and FDI output signals, which should be transmitted to the simulator computer. The torque command is generated by the recovery algorithm after fault declaration by the FDI algorithm, which should be applied to the satellite simulator model to guarantee its stability.
- *Interface circuits*: Interface circuits consist of the appropriately selected I/O cards which have the role of receiving the output states of the computer simulator and transmitting the output signals generated by the FDIR algorithm.

Figure 11 shows a real view of the mentioned elements and their connections. connected to each other.

Figure 12 depicts the test results for a scenario in which abrupt faults have occurred in each of the three reaction wheels. As this figure reveals, in spite of the faults in the reaction wheels, estimation errors of the implemented adaptive observer remains bounded. Also, the fault estimations track the real fault profiles, and so validate the fault detection and identification performances in an onboard implementation test. As seen in this figure, the fault estimations are corrupted by noise, due to the measuring sensors. To cope with this event and prevent false fault declaration, the fault estimation signals have been filtered by onboard electronics, as it was represented in Figure 12. This

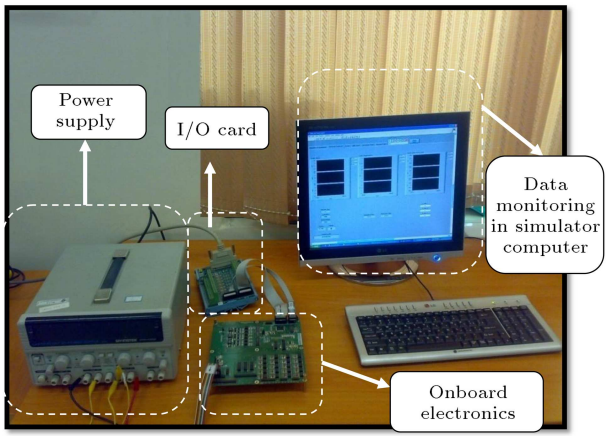

Figure 11. Hardware in the loop test facility.

figure shows that the filtered signals provide smooth profiles which are more compatible with the real fault profiles, and hence it is possible to achieve a more accurate and fine FDD process.

To evaluate the FDD performance in a case in which the FDD algorithms are exposed to a high severity of sensor noises, Figure 13 presents the fault simulator outputs in a condition where the measured signals are corrupted by a noise with the standard deviation 10^{-3} rad/sec. As the filtered signals depicted in this figure reveal, even in these harsh conditions, the fault declaration process works correctly, and the fault estimation profile tracks the real fault profile applied to the reaction wheels.

Figures 14 and 15 represent the satellite attitude angles and angular velocities achieved by the recovery algorithm implemented in the onboard electronics. Figure 14 shows the variables of interest in conditions where no compensation has been accomplished. As can be observed, an offset has appeared in the yaw axis angle (Ψ). Figure 15 depicts the results when the compensation algorithm has been activated. It is evident from this figure that despite fault existence in the actuators, the satellite maintains its stability, and no offset has appeared in the satellite states.

Table 2 indicates a comparison between simulation and experimental results of the developed recovery algorithm. As this table illustrates, there are some deviations between the results depicted. According to our expectation, the obtained results in the simulation case is somewhat better than the experimental case which is reasonable due to reasons detailed below:

1. Accuracy of the float calculations in the on-board electronics processor is more restrictive than the CPU of the simulator computer, so some deviations between the related results occur.
2. The major deviation between these two results originates from the analog to digital and digital to analog conversions.

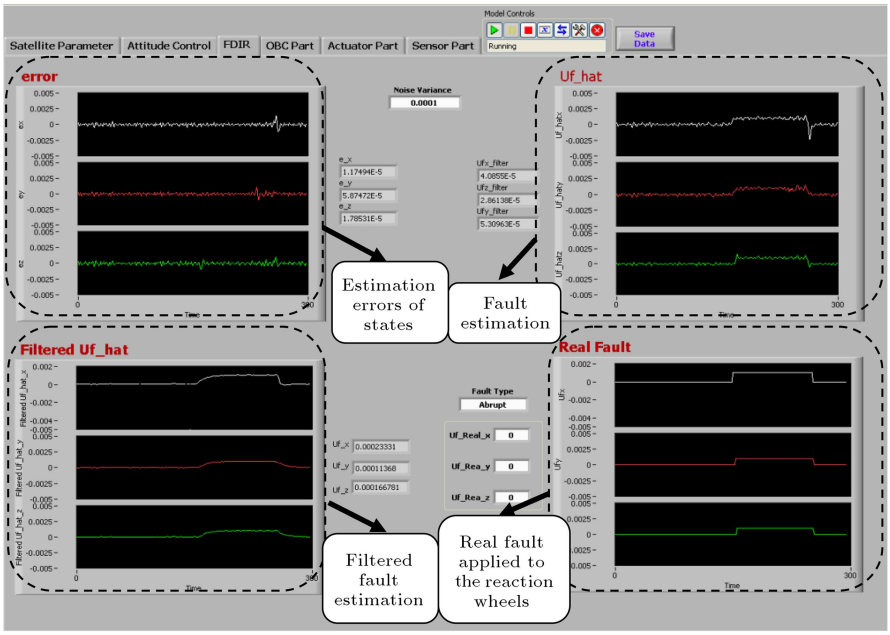

Figure 12. Fault detection and identification test results after fault occurrence in the reaction wheels.

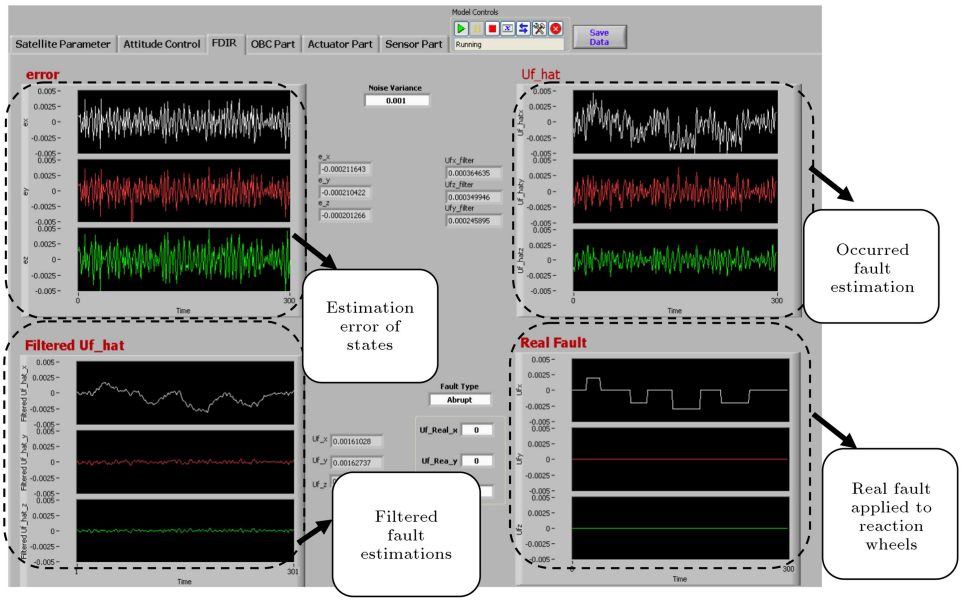

Figure 13. Fault detection and isolation test results after intermittent fault occurrence in the reaction wheel, aligned with the x axis, considering a measuring noise with the standard deviation of 10^{-3} rad/sec.

Table 2. Simulation and experimental results of the recovery algorithm.

	No fault		Fault application in all three reaction wheels with no recovery activation		Fault application in all three reaction wheels and utilizing the recovery algorithm	
	Simulation results	**Experimental results**	**Simulation results**	**Experimental results**	**Simulation results**	**Experimental results**
Roll error	0.0062°	0.09°	0.4778°	0.48°	0.0086°	0.07°
Pitch error	0.0017°	0.15°	0.4433°	0.36°	0.0023°	0.14°
Yaw error	0.0019°	0.08°	1.475°	3.20°	0.0023°	0.08°

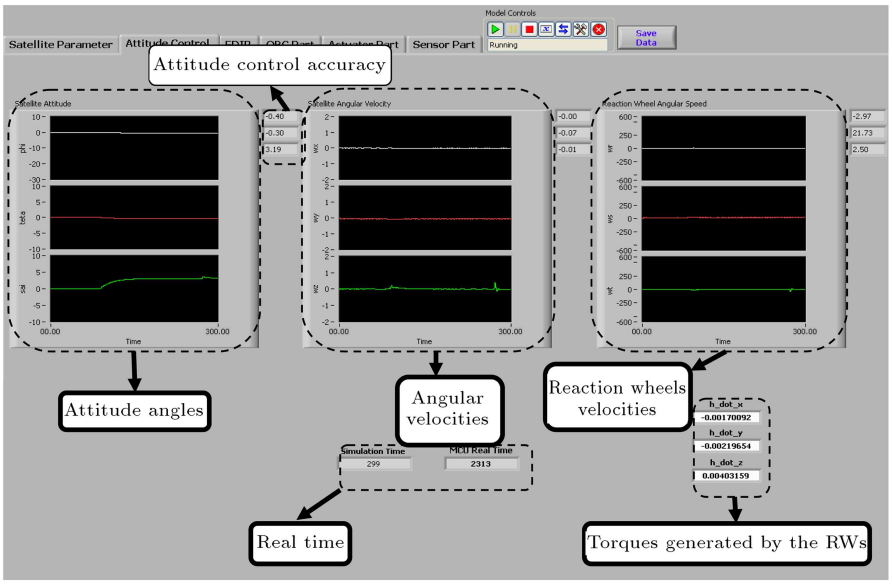

Figure 14. Satellite attitude angles after fault occurrence in each of the three reaction wheels and without fault compensation.

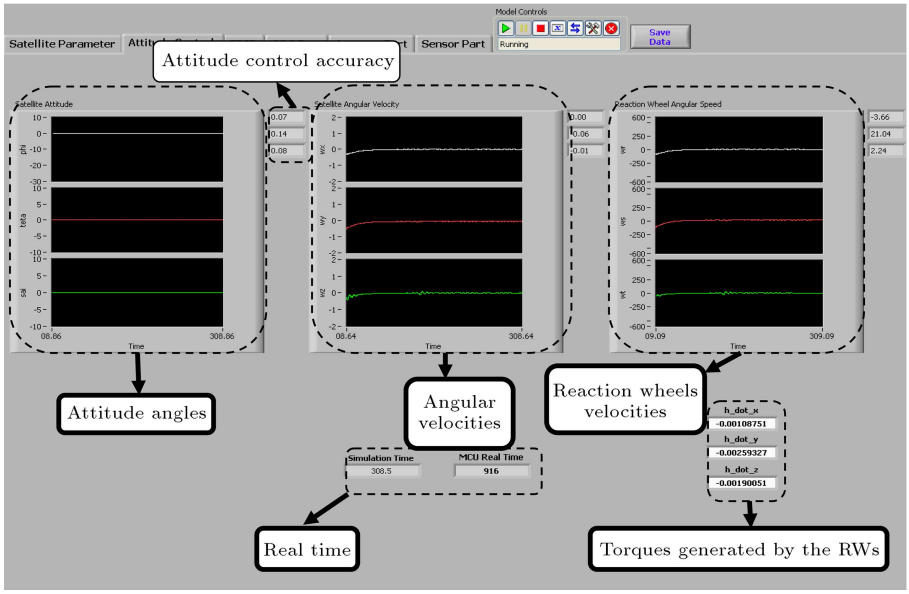

Figure 15. Satellite attitude angles after fault occurrence in each of the three reaction wheels and with activation of the fault compensating algorithm.

Since the data must be transferred between the on-board electronics and the simulator computer, a 16 bit conversion is inevitable, so this conversion error may lead to deterioration of the experimental results. Note that since in real situations there is no need to transfer data between the on- board electronics and the computer, this error is not a problem. In fact, the requested attitude determination data received directly from the attitude sensors and the generated torque by the reaction wheels is directly applied on the satellite body. As a result, although there are some deviations between simulation results and experimental results, due to the reasons stated, these deviations are not critical, and the results obtained are accurate enough for application in orbit.

8. Conclusions

This paper described both theoretical and experimental results focused on a study of fault tolerant attitude control system. The proposed FDD algorithms provide the ability of actuators fault detection, accurate identification of their magnitudes and also the isolation possibility between them. The above capabilities

were achieved under the conditions where no prior information about the fault nature was used in the FDD design process. The FDD design was evaluated using several different types of reaction wheel failure scenarios, through which the desired performance were validated taking into account the disturbances, uncertainties and unknown faults.

In this paper, also the design steps of the recovery algorithm, based on a backstepping feedback linearization controller, were presented, in which the fault magnitude estimation accomplished by the FDD algorithm was utilized. As the simulation results revealed, this algorithm provided the compensation ability of the fault effect such that no deviation of the system from the desired pointing attitude occurred. These analytical investigations demonstrated the robustness of the control design to the disturbances, measurement noise and unknown faults, and so the expected performance was achieved. To highlight the potentialities of the proposed algorithms in real applications, hardware in the loop test facility was planned to study the digital implementation of the designed algorithms, and provide more accurate and realistic results. As observed from the test results, the developed algorithms maintained their desired performances, which validated their feasibility in real-time implementations. Future work is planned to study reliability and dependability analyses which are of paramount importance for aerospace applications.

References

1. Venkateswaran, N., Siva, M.S. and Goel, P.S. "Analytical redundancy based fault detection of gyroscopes in spacecraft applications", *Acta Astronautica*, **50**(9), pp. 535-545 (2002).
2. Castet, J.F. and Saleh, J.H. "Satellite and satellite subsystems reliability: Statistical data analysis and modeling, reliability engineering and system safety", *Reliability Engineering & System Safety*, **94**, pp. 1718-1728 (2009).
3. Patton, R.J. "Fault detection and diagnosis in aerospace systems using analytical redundancy", *Computing and Control Engineering Journal*, pp. 127-136 (1991).
4. Hwang, I. and Kim, S. "A survey of fault detection, isolation and reconfiguration methods", *IEEE Transactions on Control Systems Technology*, **18**(3), pp. 636-653 (2010).
5. Frank, P.M. "Fault diagnosis in dynamic systems using analytical and knowledge-based redundancy-a survey and some new results", *Automatica*, **26**(3), pp. 459-474 (1990).
6. Iserman, R. "Model-based fault detection and diagnosis-status and applications", *Annual Reviews in Control*, **29**, pp. 71-85 (2005).
7. Venkatasubramanian, V., Rengaswamy, R. and Kavuri, S.N. "A review of process fault detection and diagnosis. Part I: Quantitative model-based methods", *Computers & Chemical Engineering*, **27**, pp. 293-311 (2003).
8. Valdes, A. and Khorasani, K. "A pulsed plasma thruster fault detection and isolation strategy for formation flying of satellites", *Applied Soft Computing*, **10**, pp. 746-758 (2010).
9. Li, Z.Q., Ma, L. and Khorasani, K. "A dynamic neural network-based reaction wheel fault diagnosis for satellites", *International Joint Conference on Neural Networks Sheraton Vancouver Wall Centre Hotel*, Vancouver, BC, Canada, pp. 3714-3721 (2006).
10. Fan, C., Jin, Z., Zhang, J. and Tian, W. "Application of multi sensor data fusion based on RBF neural networks for fault diagnosis of SAMs", *Seventh International Conference on Control, Robotics and Vision*, **3**, pp. 1557-1562 (2002).
11. Zhao, S. and Khorasani, K. "A recurrent neural network based fault diagnosis scheme for a satellite", *The 33rd Annual Conference of the IEEE Industrial Electronics Society*, Nov. 5-8, Taipei, Taiwan, pp. 2660-2665 (2007).
12. Pirmoradi, F.N., Sassani, F. and Silva, C.W.D. "Fault detection and diagnosis in a spacecraft attitude determination system", *Acta Astronautica*, **65**, pp. 710-729 (2009).
13. Okatan, A., Hajyev, C. and Hajiyeva, U. "Kalman filter innovation sequence based fault detection in Leo satellite attitude determination and control system", *3rd International Conference on Recent Advances in Space Technologies RAST '07*, Istanbul, pp. 411-416 (2007).
14. Xiong, K., Chan, C.W. and Zhang, H.Y. "Detection of satellites attitude sensor faults using the UKF", *IEEE Transactions on Aerospace and Electronics Systems*, **43**(2), pp. 480-491 (2007).
15. Soken, H.E. and Hajiyev, C. "Pico satellite attitude estimation via robust unscented Kalman filter in the presence of measurement faults", *ISA Transactions*, **49**, pp. 249-256 (2010).
16. Bae, J. and Kim, Y. "Attitude estimation for satellite fault tolerant system using federated unscented Kalman filter", *International Journal of Aeronautical & Space Science*, **11**(2), pp. 80-86 (2010).
17. Tudorou, N. and Khorasani, K. "Satellite fault diagnosis using a bank of interacting Kalman filters", *IEEE Transactions on Aerospace and Electronics Systems*, **43**(4), pp. 1334-1350 (2007).
18. Patton, R.J., Uppal, F.J., Simani, S. and Polle, B. "Robust FDI applied to thruster faults of a satellite system", *Control Engineering Practice*, **18**, pp. 1093-1109 (2010).
19. Patton, R.J., Uppal, F.J., Simani, S. and Polle, B. "Reliable fault diagnosis scheme for a spacecraft attitude control system", *Proc. IMechE, Part O: J. Risk and Reliability*, **222**, pp. 139-152 (2008).

20. Henry, D. "Robust fault diagnosis of the microscope satellite micro-thrusters", *IFAC Fault Detection, Supervision and Safety of Technical Processes*, Beijing, pp. 342-347 (2006).

21. Jiang, T. and Khorasani, K. "A fault detection, isolation and reconstruction strategy for a satellite's attitude control subsystem with redundant reaction wheels", *IEEE International Conference on Systems, Man and Cybernetics*, Montreal, Que, pp. 3146-3152 (2007).

22. Wu, L., Zhang, Y. and Li, H. "Research on fault detection for satellite attitude control systems based on sliding mode observers", *IEEE International Conference on Mechatronics and Automation*, Changchun, China, pp. 4408-4413 (2009).

23. Wu, Q. and Saif, M. "Robust fault diagnosis of a satellite system using a learning strategy and second order sliding mode observer", *IEEE Systems Journal*, **4**(1), pp. 112-121 (2010).

24. Zhang, K., Jiang, B. and Shi, P. "Adaptive observer-based fault diagnosis with application to satellite attitude control systems", *Second International Conference on Innovative Computing, Information and Control*, Kumamoto, pp. 508-508 (2007).

25. Wang, J. Jiang, B. and Shi, P. "Adaptive observer based fault diagnosis for satellite attitude control systems", *International Journal of Innovative Computing, Information and Control, ICIC International*, **4**(8), pp. 1921-1929 (2008).

26. Tanaka, K. and Wang, H.O., *Fuzzy Control System Design and Analysis*, John Wiley & Sons, pp. 5-10 (2001).

27. Sidi, M.J., *Spacecraft Dynamics and Control*, Cambridge University Press, pp. 88-95 (1997).

28. Jiang, B., Gao, Z., Shi, P. and Xu, Y. "Adaptive fault-tolerant tracking control of near-space vehicle using Takagi-Sugeno fuzzy models", *IEEE Trans. Fuzzy Systems*, **18**(5), pp. 1000-1007 (2010).

29. Ichalal, D., Marx, B., Ragot, J. and Maquin, D. "Fault tolerant control for Takagi-Sugeno systems with unmeasurable premise variables by trajectory tracking", *IEEE International Symposium on Industrial Electronics*, pp. 2097-2102 (2010)

30. Khalil, H., *Nonlinear Systems*, 2nd Ed. Upper Saddle River, NJ, Prentice-Hall, pp. 588-601 (1996).

31. Chen, C.T., *Linear System Theory and Design*, Holt, Rinehart and Winston, pp. 400-404 (1970).

Biographies

Hossein Bolandi received his DSc degree in Electrical Engineering from George Washington University, Washington, D.C., in 1990. Since 1990 he has been with the College of Electrical Engineering, Iran University of Science and Technology, Tehran, Iran, where he is an associate professor. His research interests are in attitude determination and control subsystems of satellites, adaptive control, automation and guidance, and navigation and control.

Mehran Haghparast received his BSc and MSc degrees in Electrical Engineering from Iran University of Science and Technology, Tehran, Iran in 2008 and 2011, respectively. His research interests are in attitude control subsystems of satellites, fault detection and isolation system, robust control and applied control theory.

Mostafa Abedi received his BSc degree in Electrical Engineering from the Chamran University and his MSc degree from the Iran University of Science and Technology in 2004 and 2007, respectively. He is now PhD candidate in the electrical department, Iran University of Science and Technology, Tehran. His research interests are in attitude determination of satellites, satellite sensors, fault detection and isolation.